A Facile Approach to Fabricate Porous Nylon 6 Nanofibers Using Silica Nanotemplate

Quan Shi,[1] Narendiran Vitchuli,[1] Liwen Ji,[1] Joshua Nowak,[2] Marian McCord,[1] Mohamed Bourham,[2] Xiangwu Zhang[1]

[1]*Fiber and Polymer Science Program, Department of Textile Engineering, Chemistry and Science, North Carolina State University, Raleigh, North Carolina 27695-8301*
[2]*Department of Nuclear Engineering, North Carolina State University, Raleigh, North Carolina 27695-7909*

Received 8 May 2010; accepted 9 August 2010
DOI 10.1002/app.33161
Published online 14 October 2010 in Wiley Online Library (wileyonlinelibrary.com).

ABSTRACT: Porous Nylon 6 nanofibers were prepared using silica nanoparticles as the template. Firstly, Nylon 6/silica composite nanofibers were prepared as precursors by electrospinning Nylon 6 solutions containing different contents of silica nanoparticles. Scanning electron microscopy (SEM) and transmission electron microscopy (TEM) were used to examine the surface morphology and the inner structure of composite nanofibers; where it was found that silica nanoparticles were distributed both inside and on the surface of nanofibers. Analytical techniques [Fourier transform infrared (FTIR), differential scanning calorimetry, thermal gravimetric analysis (TGA), and wide-angle X-ray diffraction) were used to study the structure and properties of these composite nanofibers. The glass transition, melting, and crystallization processes of the fibers were affected by the addition of silica nanoparticles. Secondly, porous Nylon 6 nanofibers were obtained by removing silica nanoparticles via hydrofluoric acid treatment. The removal of silica nanoparticles was confirmed using FTIR and TGA tests. SEM and TEM observations revealed the formation of the porous structure in these nanofibers. After the formation of the porous structure, Brunauer–Emmett–Teller specific surface areas of nanofibers were increased as compared to solid Nylon 6 and composite nanofibers. J Appl Polym Sci 120: 425–433, 2011

Key words: electrospinning; nanocomposite; porous nanofibers; Nylon 6

INTRODUCTION

Electrospun nanofibers are becoming a versatile category of materials for a multitude of applications.[1,2] By electrospinning, a variety of materials can be processed into nonwoven nanofiber mats with large specific surface area. The structure of these nanofibers can be easily controlled by manipulating electrospinning parameters, such as solution concentration, accelerating voltage, and flow rate.[3–6] In recent years, electrospun nanofibers research has covered a broad range of fields including, but not limited to, protective textiles,[7] tissue engineering,[8,9] homogeneous catalysis,[10] sensors,[11,12] and biomedical and biopolymer applications.[13–17]

So far, efforts have been made to control the inner structure of electrospun nanofibers to improve their properties. One popular method is to reinforce electrospun nanofibers by introducing inorganic nanoparticles. It is well known that polymer/inorganic nanocomposites can combine advantages of two distinct materials and hence lead to mechanical, electrical, and thermal properties that can be easily modified for multifunctional applications.[18–23] Among many polymer/inorganic nanocomposite systems, the preparation of polymer/silica nanofibers is a simple and universal method to improve the toughness, durability, and permeability of polymer nanofibers.[24,25] Some efforts have been reported to prepare polymer/silica composite nanofibers by the combination of sol-gel synthesis and electrospinning. PVA/silica,[26,27] PMMA/silica[28], and PEO/silica[29] composite nanofibers have also been successfully obtained by this method. Recently, the authors prepared PAN/silica composite nanofibers by electrospinning PAN solutions containing different content of silica nanoparticles without adding the sol-gel synthesis step, which presents a new and simple approach to prepare polymer/inorganic composite nanofibers.[30]

Another advantage of polymer/silica nanocomposites is that they can be used as precursor to fabricate nanoporous nanofibers by removing silica nanoparticles. Porous nanofibers, which have extra high specific surface area and porosity, are expanding the application scope of nanofibers in membranes, filters, sensors, and coatings.[31,32] Porous fibers were prepared by several groups by electrospinning bicomponent polymer blends then selectively

Correspondence to: X. Zhang (xiangwu_zhang@ncsu.edu).
Contract grant sponsor: Defense Threat Reduction Agency; contract grant number: BB08PRO008.

removing one of them.[33,34] Porous structures can also be obtained in nanofibers by controlling the humidity or molecular weight in the one-component electrospinning.[35] Nylon 6 is one of the most widely used polymer materials in protective and filter fabrics. Porous structure in Nylon 6 fibers can improve their surface area and hence the filtration efficiency and catalyst-loading capacity. Recently, Gupta et al.[36] have exploited a new approach to produce porous nanofibers by electrospinning the Lewis acid–base complex of Nylon 6 and $GaCl_3$, referred to as the "salt-induced" process. All these methods require handling complicated interactions between the polymer matrix and pore generator, such as the secondary polymer, moisture, and salt. Compared with the existing methods, removing silica nanoparticles from composite nanofibers is a relatively simple process. This pore formation process is decoupled from the polymer-silica interaction. In addition, the porosity and pore size of the resultant porous nanofibers can be easily controlled by adjusting the content and size of silica nanoparticles.

The aim of this research is to establish a simple and efficient method to fabricate porous Nylon 6 nanofibers using silica nanoparticles as the template. In this work, we first prepared Nylon 6/silica composite nanofibers by the electrospinning of Nylon 6 solutions containing different contents of silica nanoparticles. Characterization of the effects of silica particles on the structure of nanofibers was performed. Silica nanoparticles were then removed from the composite nanofibers through treatment with hydrofluoric (HF) acid solution. Surface morphology, specific surface area, thermal properties, and crystal structure of the composite and porous fibers were investigated.

EXPERIMENTAL

Materials

Nylon 6, solvent 2,2,2-tri-fluoroethanol (TFE), and HF acid (35% in H_2O solution) were purchased from Sigma-Aldrich. Silica nanoparticles (AEROSIL® 380, average primary particle size = 7 nm, and specific surface area = 380 ± 30 m^2/g) were supplied by Evonik Degussa GmbH (Essen, Germany). All these reagents were used without further purification.

Electrospinning

Nylon 6 was dissolved in TFE at a concentration of 13 wt % to get a stock solution. Weighed silica nanoparticles were dispersed in the solution by magnetic stirring at 45°C for 24 h to get a homogeneous mixture. The resultant mixture was agitated in an ultrasonic bath for 15 min before electrospinning. Electrospinning uses a high-voltage power supply (Gamma ES40P-20W/DAM), which provided 15 kV during these experiments. A plastic syringe attached with a stainless steel needle tip was used to load the electrospinning solution. The syringe was controlled by an electric pump to obtain a fixed feed rate of 1.5 mL/h. The needle was charged with positive voltage and the metal collector was grounded, and the distance between the needle and collector was 15 cm. The electrospun fibers were collected on the aluminum foil on the collector as a fibrous mat.

Formation of porous structure

A HF acid solution of 10 wt % was obtaining by diluting the commercial HF solution (35 wt %) with deionized water. Nanofiber mats were cut into 2 × 2 in pieces and weighed precisely. Nanofiber mats were then immersed into the HF solution and kept for 24 h. Afterward, nanofiber mats were washed three times with deionized water, dried by vacuum, weighed, and collected for further use.

Morphology

Surface morphology of nanofibers was observed by JEOL JSM-6400F field emission scanning electron microscopy (SEM; JEOL, Tokyo, Japan), with an accelerating voltage of 15 kV. The distribution of silica nanoparticles and pores inside the fibers were observed using a Hitachi HF-2000 transmission electron microscopy (TEM; Hitachi High Technologies America), with an accelerating voltage of 20 kV.

Surface analysis

Information about the surface composition of the nanofibers was obtained by collecting attenuated total reflection Fourier transform infrared (ATR-FTIR) spectra on a Nicolet 560 FTIR spectrometer. The tests were performed in the wave number range of 3750–750 cm^{-1} at room temperature.

Thermal analysis

Thermal properties of electrospun fibers were measured by differential scanning calorimetry (DSC; Perkin–Elmer Diamond). The measurements were carried out under nitrogen atmosphere in a temperature range between −20 and 250°C, at a heating rate of 20°C/min. Thermal decomposition properties of electrospun fibers at elevated temperatures was assessed by thermal gravimetric analysis (TGA; TA Hi-Res 2950). The tests were performed in the temperature range of 25–800°C under nitrogen atmosphere at a heating rate of 20°C/min.

Crystal structure

Crystal structure of the composite and porous fibers was characterized by wide-angle X-ray diffraction (WAXD). Spectra were collected on a Philips XLF

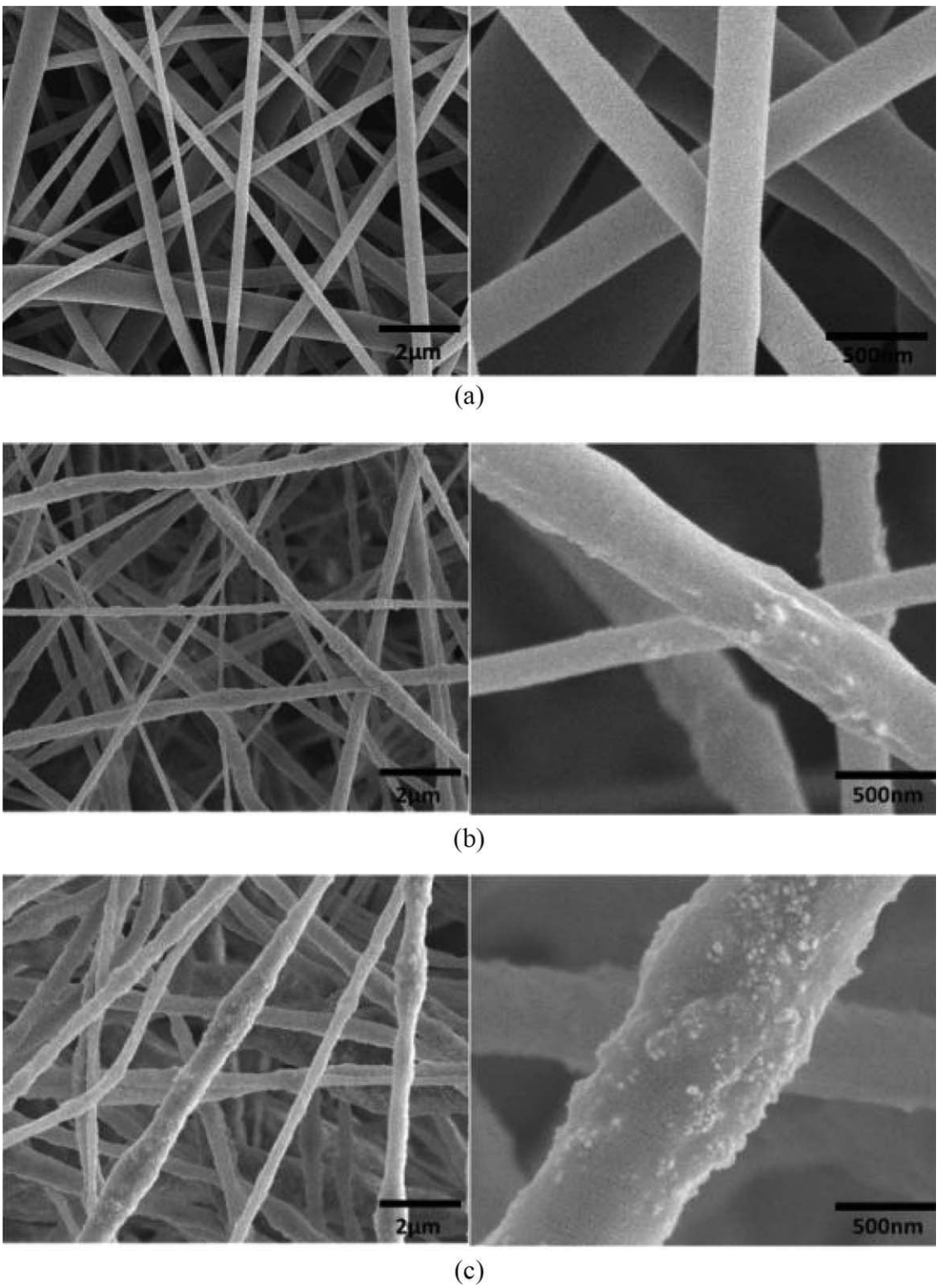

Figure 1 SEM images of Nylon 6 and Nylon 6/silica composite nanofibers. Silica content: (a) 0, (b) 15, and (c) 30 wt %.

ATPS XRD 100 diffractometer (Cu Kα radiation). The operating voltage was 40.0 kV, and the current was 60.0 mA. Data were collected at the interval of 0.02° and the scanning rate of 1 s/step. Peak positions were determined by the APD 1700 (Version 4) software.

Surface specific area analysis

Surface specific areas of the composite and porous nanofibers were determined by Brunauer–Emmett–Teller (BET) nitrogen adsorption method. The samples were first stabilized in nitrogen atmosphere for 2 h at

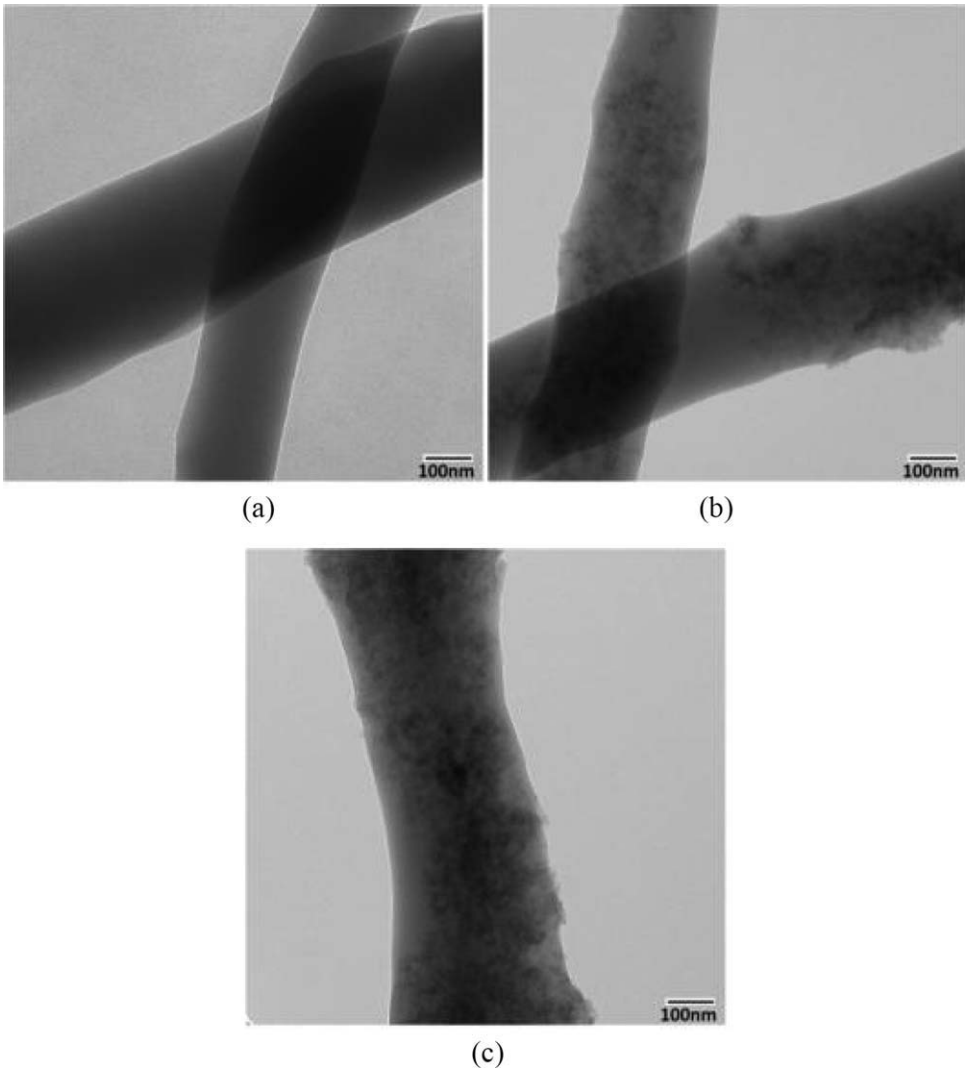

Figure 2 TEM images of Nylon 6 and Nylon 6/silica composite nanofibers. Silica content: (a) 0, (b) 15, and (c) 30 wt %.

50°C. Nitrogen gas adsorption measurements were taken at 5, 10, 15, 20, and 25% of saturation pressure on a Micromeritics Gemini 2360 instrument capable of measuring surface area of 0.01 m^2 g^{-1} and higher.

RESULTS AND DISCUSSION

Electrospun Nylon 6/silica composite nanofibers

Nylon 6/silica composite nanofibers containing 15 and 30 wt % silica particles were obtained by electrospinning. SEM images show the surface morphology of Nylon 6 nanofibers (0, 15, and 30 wt % silica nanoparticles; Fig. 1). It is clear from the low-magnification images that pure Nylon 6 nanofibers have smooth and continuous fibrous structures, with diameters ranging between 200 and 400 nm. Nylon 6/silica nanofibers have a rough surface, which may to be attributable to aggregation of some of the silica nanoparticles. The addition of highly surface-active silica nanoparticles can increase both the viscosity and surface tension of electrospinning solutions, which may also contribute to the increased surface roughness of composite nanofibers.[37] The diameters of the 30 wt % composite nanofibers are generally larger than those of 0 and 15 wt % nanofibers.

The high-magnification SEM images in Figure 1 reveal that increasing silica content results in more silica nanoparticles appearing on the surfaces of the fibers. TEM images provide detailed information on the inner structure of Nylon 6/silica composite nanofibers (Fig. 2). Pure Nylon 6 fibers were uniform in composition from the center to the surface. In the Nylon 6/silica composite nanofibers, silica nanoparticles were found distributed all over the fiber matrix. It can be seen that there are some silica nanoparticles aggregating at a few locations. The TEM results agree with SEM images.

FTIR and TGA analyses of Nylon 6/silica composite nanofibers

The ATR-FTIR spectra are shown in Figure 3. The FTIR spectrum (curve a) of Nylon 6 nanofibers

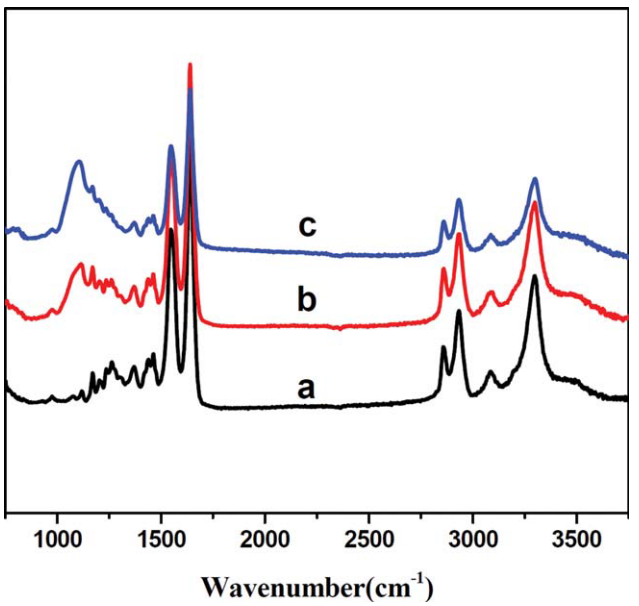

Figure 3 FTIR spectra of Nylon 6 and Nylon 6/silica composite nanofibers. Silica content: (a) 0, (b) 15, and (c) 30 wt %. [Color figure can be viewed in the online issue, which is available at wileyonlinelibrary.com.]

presents typical peaks at 1547 cm^{-1} (N—H deformation), and 1636 cm^{-1} (C=O stretch), 3292 cm^{-1} (N—H stretch). These peaks can also be found in the spectra for the 15 and 30 wt % Nylon 6/silica composite nanofibers (curves b and c). The most significant difference in the spectra is the peak at 1100 cm^{-1}, which is the characteristic signal of Si—O—Si bond asymmetric stretching vibration and only exists in composite nanofibers.[22]

Results of the TGA studies were used to assess the actual content of silica nanoparticles in composite nanofibers (Fig. 4). Pure Nylon 6 fibers give nearly 0 wt %

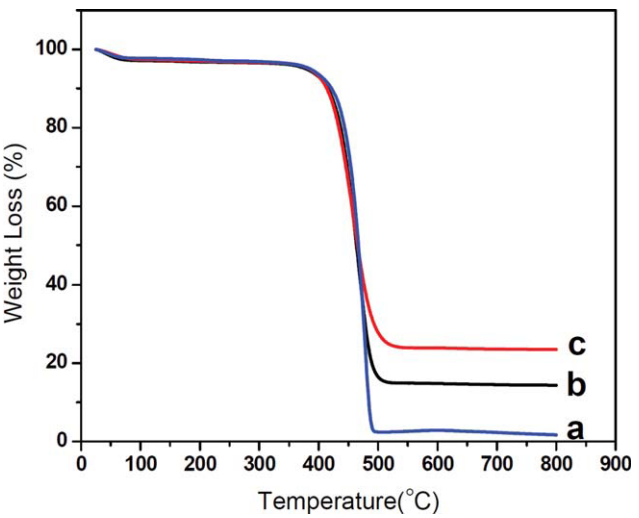

Figure 4 TGA thermograms of Nylon 6 and Nylon 6/silica composite nanofibers. Silica content: (a) 0, (b) 15, and (c) 30 wt %. [Color figure can be viewed in the online issue, which is available at wileyonlinelibrary.com.]

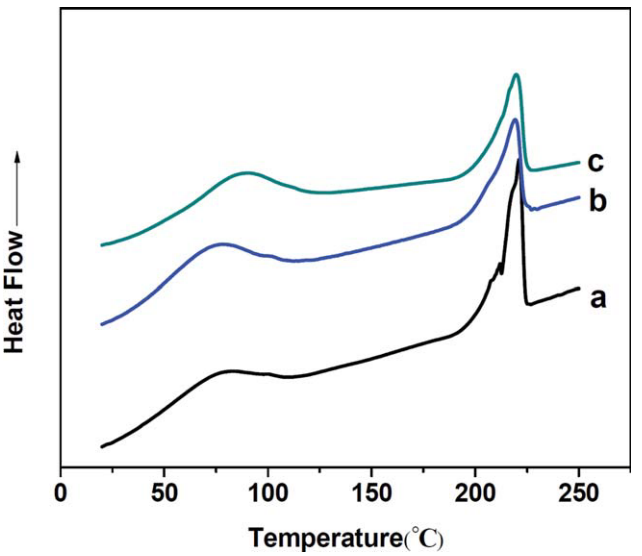

Figure 5 DSC Thermograms of Nylon 6 and Nylon 6/silica composite nanofibers. Silica content: (a) 0, (b) 15, and (c) 30 wt %. [Color figure can be viewed in the online issue, which is available at wileyonlinelibrary.com.]

residuals after the temperature increased to 800°C as indicated in curve a. The 15 and 30 wt % composite nanofibers contain 15.0 and 23.9% residuals, as shown in curves b and c, respectively; this indicates the actual silica content in the composite nanofibers.

Thermal properties and crystalline structure of Nylon 6/silica composite nanofibers

The DSC curves of both pure Nylon 6 fibers and Nylon 6/silica composite nanofibers are shown in

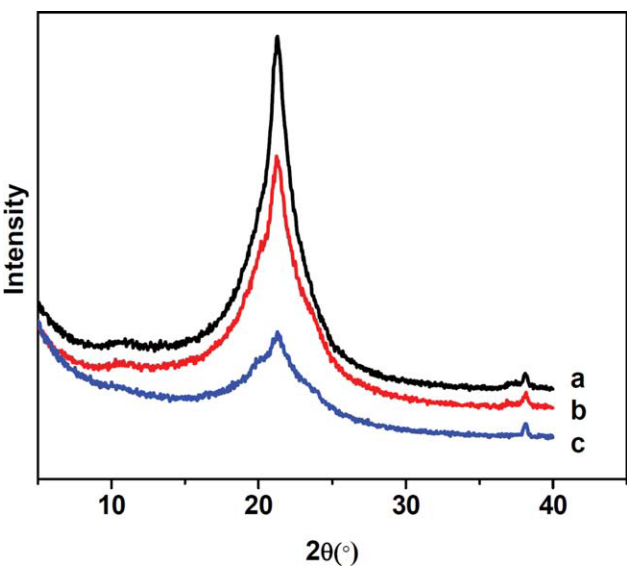

Figure 6 WAXD spectra of Nylon 6 and Nylon 6/silica composite nanofibers. Silica content: (a) 0, (b) 15, and (c) 30 wt %. [Color figure can be viewed in the online issue, which is available at wileyonlinelibrary.com.]

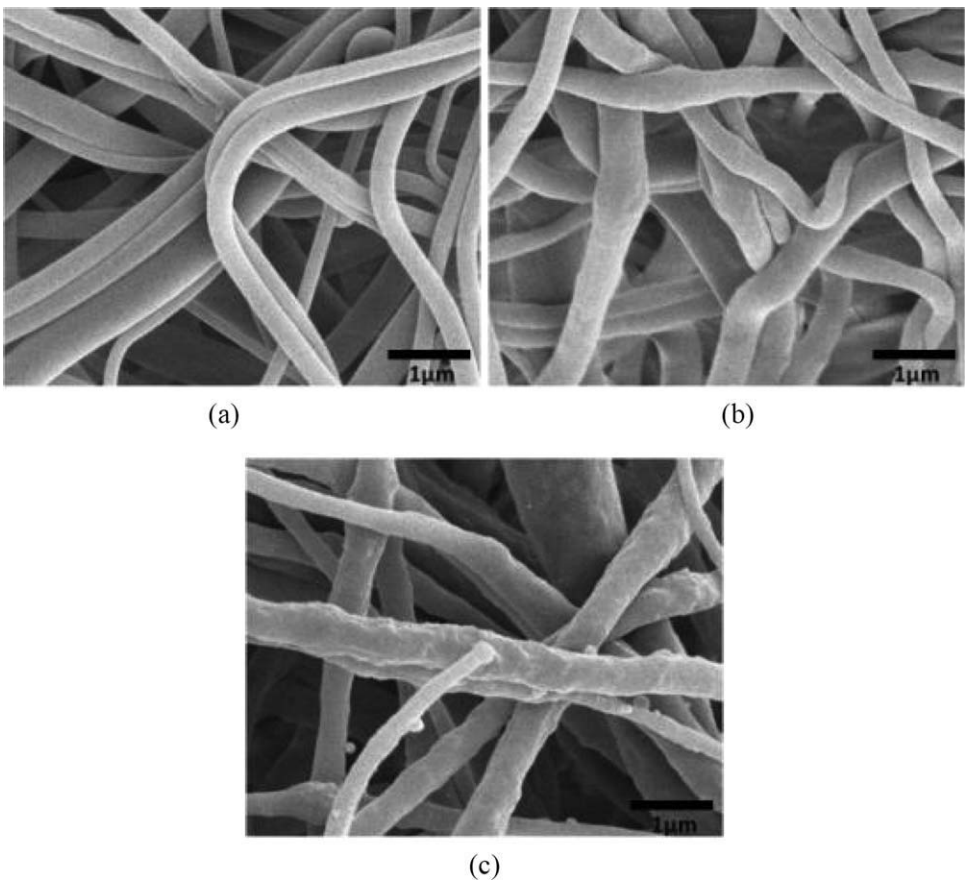

Figure 7 SEM images of Nylon 6 and Nylon 6/silica composite nanofibers after the treatment with 10% HF solution for 24 h. Silica content: (a) 0, (b) 15, and (c) 30 wt %.

Figure 5. It is clear that the glass transition temperature (T_g) of nanofibers increases with increasing content of silica nanoparticles. This indicates that the highly active surface of silica nanoparticles can form interactions with the polymer chains.[38] Silica nanoparticles used in this work are hydrophilic and have a large amount of surface hydroxyl groups (2.5 —OH/nm^2).[39] Most likely the interactions occur between these hydroxyl groups and oxygen/nitrogen atoms on Nylon molecules. The hydrogen bonds formed between silica and Nylon 6 hinder the movements of polymer chains and increase the glass transition temperature T_g.

It is also seen from Figure 5 that the crystallinity of nanofibers is also affected by the addition of silica nanoparticles. Nylon 6 nanofibers show a characteristic melting exotherm at 219°C. Nylon 6/silica composite nanofibers have melting exotherms at slightly lower temperatures.

To understand the nanofiber structure, WAXD diffraction patterns of Nylon 6 and Nylon 6/silica composite fibers were collected and are shown in Figure 6. All nanofibers show a diffraction peak at $2\theta = 22°$, which is the characteristic peak for Nylon 6. With the increase in the silica content, the intensity of the peak at $2\theta = 22°$ decreases. This indicates that the crystallinity of Nylon 6 in the composite nanofibers is remarkably lowered by the introduction of silica nanoparticles. As there are no chemical changes to the polymer molecules, the decrease in crystallinity can be attributed to the interaction between silica nanoparticles and polymer chains, which may hinder the alignment of polymer chains during the crystallization process.

Preparation of porous Nylon 6 nanofibers

Porous Nylon 6 nanofibers were prepared using Nylon 6/silica composite nanofibers as the precursor. Composite nanofibers were treated by 10 wt % HF acid water solution to remove the silica particles. Pure Nylon 6 nanofibers were also treated by HF under the same conditions as a control. Figure 7 shows the SEM images of the treated fibers. After treatment, pure Nylon 6 nanofibers remain smooth with a continuous fibrous structure, showing similar morphology to the untreated ones [Fig. 1(a)]. The HF-treated 15-wt % nanofibers [Fig. 7(b)] have a relatively large morphology change as compared to the untreated ones [Fig. 1(a)], that is, their surface

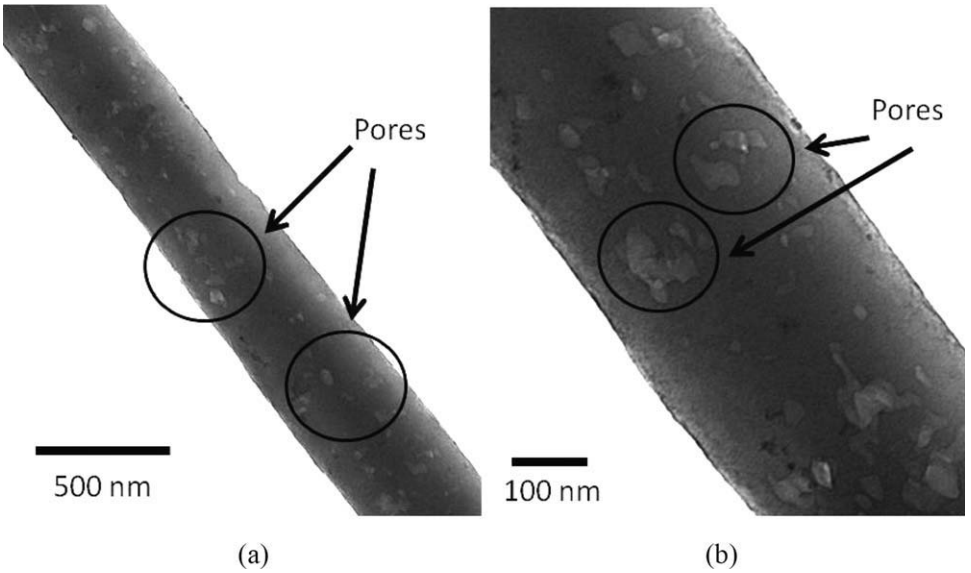

Figure 8 TEM images of porous Nylon 6 nanofibers prepared by treating 30 wt % Nylon 6/silica composite nanofibers with 10% HF solution for 24 h. Magnification: (a) 15000× and (b) 30000×.

becomes much smoother after the removal of silica nanoparticles. In the case of HF-treated 30-wt % nanofibers [Fig. 7(c)], the nanoparticles are also removed, but the fiber surface remains rough due to the high silica content in the untreated precursor fibers.

The SEM images are too low in resolution to reveal details about the pore structures within the fibers, however, the pores can be observed in the TEM images (Fig. 8). Large numbers of pores with sizes varying from several to dozens of nanometers can be seen in Nylon 6 nanofibers obtained after removing silica from 30 wt % Nylon 6/silica precursor. The formation of the porous structure is expected to greatly increase the specific surface area of the electrospun Nylon 6 nanofiber mats, which will be discussed in "Surface area and pore volume of composite and porous fibers" section.

FTIR and TGA analyses of porous Nylon 6 nanofibers

Figure 9 shows the ATR-FTIR spectra of 30 wt % composite nanofibers before and after treatment with HF solution, respectively. The absorption peak at 1100 cm^{-1}, which is attributed to Si—O—Si bond asymmetric stretching vibration, disappears after the treatment, indicating the removal of silica nanoparticles. The FTIR spectrum of pure Nylon 6 nanofibers is shown for comparison. All absorption peaks of HF-treated composite fibers are almost identical to those of the pure Nylon 6 fibers.

As shown in Figure 10, the HF-treated 30 wt % Nylon 6/silica composite nanofibers exhibit nearly 0 wt % residual at 800°C, whereas the untreated composite nanofibers have 23.9% residual. This indicates that most of the silica nanoparticles have been removed during the HF treatment.

Surface area and pore volume of composite and porous fibers

Results of the BET analyses of pure Nylon 6 nanofibers, 15 wt % Nylon 6/silica composite nanofibers, and porous nanofibers prepared by removing silica

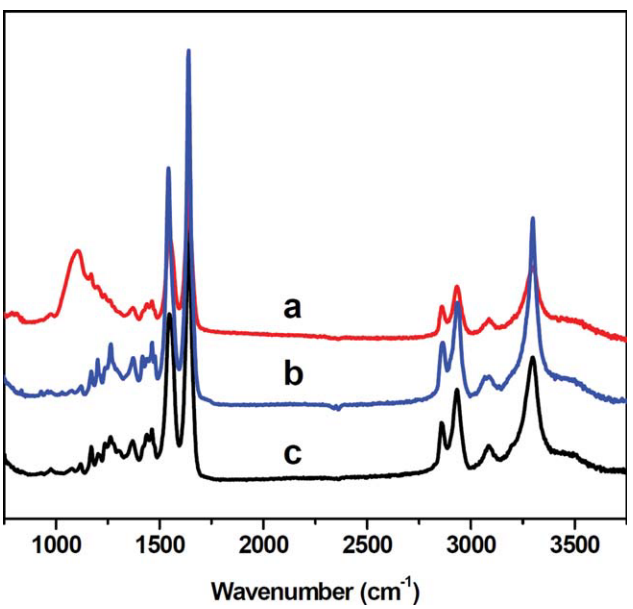

Figure 9 FTIR spectra of 30 wt % silica/Nylon 6 composite fibers before (a) and after (b) the treatment with 10% HF solution. For comparison, FTIR spectrum of pure Nylon 6 nanofibers is also shown. [Color figure can be viewed in the online issue, which is available at wileyonlinelibrary.com.]

nanoparticles from 15 wt % composite nanofibers are listed in Table I. The 15% Nylon 6/silica composite nanofibers have slightly smaller surface areas and pore volumes than the pure Nylon 6 nanofibers, which may be attributed to the electrospinning process. The viscosity of the electrospinning solution increases with the addition of silica nanoparticles. As a result, under the same electrospinning condition, composite nanofibers have slightly larger average diameters than pure Nylon 6 nanofibers (Fig. 1), and consequently, the surface area decreases in composite nanofibers. However, after the removal of silica nanoparticles, both the surface specific areas and pore volumes increase. As shown in Table I, the specific surface area increases by 162% (from 3.17 to 8.31 m^2/g). In addition, the surface area of pores increases by 174% (from 2.34 to 6.41 m^2/g) and the pore volume increases by 232% (from 0.0075 to 0.0240 cm^3/g), which indicate that the increased specific surface area is mainly a result of the generation of pores. These results, especially the pore volume data, suggest that a porous structure can be prepared by the removal of silica nanoparticles from Nylon/silica composite nanofiber. Porous nanofibers prepared by this method can have enormous potential applications such as sensors, protective fabrics, filters, and catalysts. Future work will focus on the exploration of porous nanofibers in these applications.

CONCLUSIONS

Porous Nylon 6 nanofibers were fabricated using silica nanoparticles as a the template. Nylon 6/silica composite nanofibers as precursors were prepared by the electrospinning method. SEM and TEM observations confirm the homogeneous distribution of silica nanoparticles in electrospun composite fibers. DSC, TGA, and WAXD analysis results indicate that silica nanoparticles interact with the polymer to cause significant changes in morphology. It is also demonstrated that these interactions affect the thermal properties and crystallization behavior of Nylon 6 nanofibers. Porous Nylon 6 nanofibers were then prepared by treating composite nanofibers using HF solution. ATR-FTIR and TGA tests show that the silica nanoparticles have been successfully removed from the nanofibers. Analysis of SEM and TEM images confirms the formation of the porous structure. BET specific surface area measurement reveals a 162% increase of specific surface area after the removal of silica nanoparticles. Pore volume also increased in the porous nanofibers. The structure of such fabricated porous nanofibers indicates that they have potential applications in sensors, protective fabrics, filters, and catalysts.

TABLE I
BET Surface Area Analyses of Nylon 6 Nanofibers, Nylon 6/Silica Composite Nanofibers, and Porous Nylon 6 Nanofibers

	BET surface area (m^2/g)	Surface area of pores (1.7–300 nm) (m^2/g)	Pore volume (cm^3/g)
Nylon 6 nanofibers	4.68	3.68	0.0133
15 wt% Nylon 6/silica composite nanofibers	3.17	2.34	0.0075
Porous Nylon 6 nanofibers prepared from 15% composite precursor	8.31	6.41	0.0250

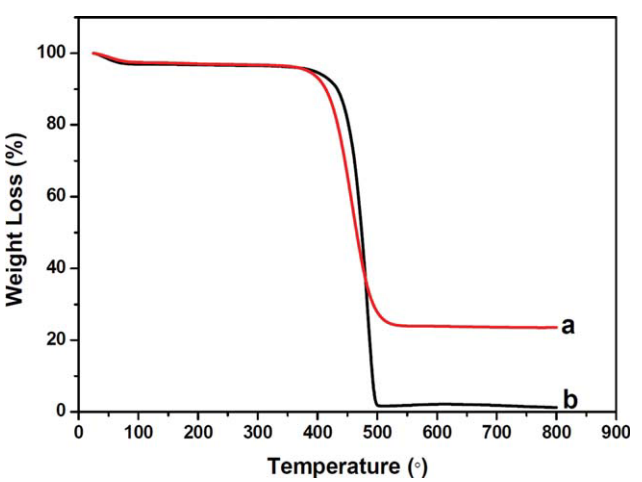

Figure 10 TGA Thermograms of 30 wt % silica composite fibers before (a) and after (b) the treatment with 10% HF solution. [Color figure can be viewed in the online issue, which is available at wileyonlinelibrary.com.]

References

1. Li, D.; Xia, Y. Adv Mater 2004, 16, 1151.
2. Kotek, R. Polym Rev 2008, 48, 221.
3. Hagewood, J.; Wilkie, A. Nonwovens World 2003, 12, 69.
4. Deitzel, J. M.; Kleinmeyer, J.; Harris, D.; Beck Tan N. C. Polymer 2001, 42, 261.
5. Frenot, A.; Chronakis, I. S. Curr Opin Colloid Interface Sci 2003, 8, 64.
6. Bellan, L. M.; Craighead, H. G. J Manuf Sci Eng-Trans ASME 2009, 131, 4.
7. Schreuder-Gibson, H.; Gibson, P.; Senecal, K.; Sennett, M.; Walker, J.; Yeomans, W.; Ziegler, D.; Tsai, P. P. J Adv Mater 2002, 34, 44.
8. Liao, S.; Li, B.; Ma, Z.; Wei, H.; Chan, C.; Ramakrishna, S. Biomed Mater 2006, 1, R45.
9. Boudriot, U.; Dersch, R.; Greiner, A.; Wendorff, J. H. Artif Organs 2006, 30, 785.
10. Michael, S.; Caren, R.; Nadine, R.; Florian, S.; Armido, S.; Andreas, G.; Joachim, H. W. Polymer 2007, 48, 5208.
11. Wang, X.; Drew, C.; Lee, S. H.; Senecal, K. J.; Kumar, J.; Samuelson, L. A. J Macromolecular Sci A 2002, 39, 1251.
12. Li, Z. Y.; Zhang, H. N.; Zheng, W.; Wang, W.; Huang, H. M.; Wang, C.; MacDiarmid, A. G.; Wei, Y. J Am Chem Soc 2008, 130, 5036.

13. Reneker, D. H.; Yarin, A. L.; Zussman, E.; Xu, H. Adv Appl Mech 2007, 41, 44.
14. Agarwal, S.; Wendorff, J. H.; Greiner, A. Polymer 2008, 49, 5603.
15. Schiffman, J. D.; Schauer, C. L. Polym Rev 2008, 48, 317.
16. Seema, A.; Andreas, G.; Joachin, H. W. Adv Funct Mater 2009, 19, 1.
17. Yang, D. Y.; Niu, X.; Liu, Y. Y.; Wang, Y.; Gu, X.; Song, L. S.; Zhao, R.; Ma, L. Y.; Shao, Y. M.; Jiang, X. Y. Adv Mater 2008, 20, 4770.
18. Sawicka, K. M.; Gouma, P. J Nanopart Res 2006, 8, 769.
19. Huang, Z. M.; Zhang, Y. Z.; Kotaki, M.; Ramakrishna, S. Compos Sci Technol 2003, 63, 2223.
20. Jie, B.; Yaoxian, L.; Meiye, L.; Junlong, G.; Xinmin, Z.; Shugang, W.; Chaoqun, Z.; Qingbiao, Y. Colloids Surf A Physicochem Eng Asp 2008, 318, 259.
21. Yongzhi, W.; Yaoxian, L.; Songtao, Y.; Guangliang, Z.; Dongmin, A.; Ce, W.; Qingbiao, Y.; Xuesi, C.; Xiabin, J.; Yen, W. Nanotechnology 2006, 17, 3304.
22. Pavan Kumar, V. S.; Jagadeesh Babu, V.; Raghuraman, G. K.; Dhamodharan, R.; Natarajan, T. S. J Appl Phys 2007, 101, 4.
23. Kim, H. W.; Lee, H. H.; Knowles, J. C. J Biomed Mater Res A 2006, 79, 643.
24. Hassan, M.; Mohammad, H.; Vinod, D.; Graham, B.; Justin, S.; Vijaya, R.; Xin, W.; Valery, K.; Shaik, J. Nanotechnology 2008, 19, 445702.
25. Zhao, C.; Zhang, P.; Lu, S.; He, J.; Wang, X. J Mater Sci 2007, 42, 9083.
26. Shao, C.; Kim, H.; Gong, J.; Lee, D. Nanotechnology 2002, 13, 635.
27. Jin, Y.; Yang, D. Y.; Kang, D. Y.; Jiang, X. Y. Langmuir 2010, 26, 1186.
28. Yi-zhang, C.; Zhan-peng, Z.; Jian, Y.; Zhao-Xia, G. J Polym Sci B Polym Phy 2009, 47, 1211.
29. Lim, J.-M.; Yi, G.-R.; Moon, J. H.; Heo, C.-J.; Yang, S.-M. Langmuir 2007, 23, 7981.
30. Liwen, J.; Carl, S.; Saad, A. K.; Xiangwu, Z.; Nanotechnology 2008, 19, 085605.
31. Michael, B.; Wolfgang, C.; Thomas, F.; Andreas, S.; Michael, H.; Martin, S.; Andreas, G.; Joachim H. W. Adv Mater 2001, 13, 70.
32. Megelski, S.; Stephens, J. S.; Chase, D. B.; Rabolt, J. F. Macromolecules 2002, 35, 8456.
33. Zhang, L.; Hsieh, Y. Nanotechnology 2006, 17, 4416.
34. Mikhail, B.; Thomas, F.; Martin, S.; Andreas, G.; Joachim, H. W. Polym Eng Sci 2001, 41, 982.
35. Casper, C. L.; Stephens, J. S.; Tassi, N. G.; Chase, D. B.; Rabolt, J. F. Macromolecules 2003, 37, 573.
36. Gupta, A.; Saquing, C. D.; Afshari, M.; Tonelli, A. E.; Khan, S. A.; Kotek, R. Macromolecules 2008, 42, 709.
37. Fong, H.; Chun, I.; Reneker, D. H. Polymer 1999, 40, 4585.
38. Arrighi, V.; McEwen, I. J.; Qian, H.; Serrano Prieto, M. B. Polymer 2003, 44, 6259.
39. Basic Characteristics of AEROSIL®, Degussa Technical bulletin Pigments Number 11, 2003.